Computational insights into the agonist activity of Cannabinoid receptor type-2 ligands using molecular dynamics simulation

Vivek Kumar Yadav[1]

Department of Chemistry, School of Advanced Sciences & Languages, VIT Bhopal University, Bhopal, MP, India 466114

Abstract

Cannabinoid (CB) receptors belong to the G protein-coupled receptor (GPCR) family and were activated by endogenous, phytogenic, and synthetic modulators. These cannabinoid receptors involved in a variety of physiological processes, including appetite, pain-sensation, mood, memory, etc. The potency of ligands with receptors provides the path with which the receptors show agonist, antagonist, or inverse agonist behavior. Due to the unavailability of the crystal structure of CB receptor type-2, we used multiple template comparative homology modeling algorithms to construct 3D models for CB2. We performed docking and molecular dynamics simulation study of four synthetic drugs in both CB1 and CB2 receptors. These ligands show agonist activity with the CB2 receptor and activate them thoroughly, and the results are compared with the CB1 receptor. Molecular properties of the ligands, including molecular, polar, and solvent accessible surface areas, and intra-molecular hydrogen bonds are evaluated throughout molecular dynamics simulations. Our finding demonstrates that the ligand AM-1221 shows the highest binding affinity -12.73 Kcal/mol whereas UR-144 shows the lowest -9.83 Kcal/mole towards the CB2 receptor. These findings should stimulate the design of ligands with distinct pharmacological properties associated with cannabinoid receptor type-2.

*Corresponding author
Email address: vivek@vitbhopal.ac.in (Vivek Kumar Yadav)
URL: https://vivekchem.wixsite.com/mysite (Vivek Kumar Yadav)

Keywords: Cannabinoid receptors (CB1 and CB2), Induced fit docking, Molecular dynamics simulations

1. Introduction

Owing to the unique behavioral, Cannabinoids have been the focus of extensive chemical and biological research[1]. Cannabinoid receptor in mammalian tissues is expressed in either CB1 or CB2, as both belong to G-protein coupled receptor and these receptors also behave as inverse agonist, which indicates that CB1 and CB2 receptors can exist in a constitutively active state. In early 1970, the research exploring the psychotropic effects of cannabis are composed primarily by trans-Δ-9-tetrahydrocannabinol (Δ-9 THC) and in 1980's it reaches to clinics. In general, cannabinoid receptors belong to those class of receptor which respond to the cannabinoid drugs. Cannabis (also known as marijuana) sativa [1, 2, 3] and its biological active synthetic analog such as Δ 9-tetrahydrocannabinol (THC) belongs to this class. The significant role of cannabinoid receptors is to repress neurotransmitter release in the brain. Tetrahydrocannabinol (THC) is the primary psychoactive compound [4, 5] found in cannabis and some other plants. In addition to THC, another major constituent from plants is Cannabidiol (CBD) which is non-psychoactive cannabinoid. Like tranquilizer, cannabinoids also affect the person directly by interacting with the specific receptors which are located within the central nervous system. These two cannabinoid receptors are termed as central cannabinoid CB1 (brain receptor) and peripheral cannabinoid CB2 (body/immune system receptor). CB1 receptors are expressed predominantly at nerve terminals where they mediate inhibition of transmitter release whereas, CB2 receptors are found mainly on immune cells. The major difference between CB1 and CB2 receptors is the difference between their amino acid sequence, their signaling mechanism and in tissue distribution.

The structure of CB1 and CB2 comprise with seven transmembrane spanning domains as commonly seen in G protein-coupled receptors[6]. Class A GPCRs

have a common topology which includes an extracellular N-terminus with a transmembrane core that is formed by a bundle of seven transmembrane α-helices (TMH1–7), three extracellular (EC) and three intracellular (IC) loops that connect these helices, and an intracellular C-terminus[7, 8, 9, 10]. CB2 has a glycosylated N-terminus, and an intracellular C-terminus, where the C-terminal of CB2 plays a critical role inducing the receptor to become less responsive to certain ligands. Human CB2 receptor consists of approximately 360 amino-acids which are somehow 25% less compared with the CB1 receptor. The CB2 receptor is liable for the anti-inflammatory and other therapeutic effects of cannabis detected in animal's model[11]. Originally it was believed that CB2 receptor was present primarily in the immune cell but later it has been reported that CB2 receptor is localized neuronally in distinct species. Different type of compound mainly targeting CB2 have been discovered and shows selective CB2 agonist activity[12, 13]. CB2 receptor plays vital therapeutic roles specifically with agonist JWH-015 in the cure of neurodegenerative disorder like Alzheimer's disease [14, 15] as this combination urge macrophage which expels indigenous beta-amyloid protein from human tissues[16].

It was found that some of the cannabinoids ligands agonist activates the CB1 and CB2 receptors with similar strength. Recently, it is concluded from ligand-protein binding affinity, that CB2 agonist ligands interacts with the receptor site in different fashion implying different binding and functional properties which is well represented by pharmacodynamic concept[17, 18, 19, 20]. CB2 receptors are asserted in various type of inflammatory cells and immunocompetent cell. An antinociceptive response is generated in the position of inflammatory hyperalgesia and neuropathic pain[21, 22] due to the activation of peripheral CB2 receptors. The mechanism which governs this CB2-mediated effect is due to the generation of inflammatory hyperalgesia[23]. In general, it is considered that CB1 receptors activation is related to the central side effects which include ataxia and catalepsy whereas selective CB2 receptor agonist potentially treat the pain without causing the side effects. In addition to above, CB2 receptors have novel pain control actions. A CB2 induced cannabinoids compounds can

inflict hyperalgesia of diversified origins and play a vital role even in neuropathic pain[24], which are conditions often refractory to analysis.

In this work, we are exclusively focusing on the interaction of four synthetic illicit drugs with Cannabinoids type-1 and type-2 receptor. According to US Department of Health and Human Services, By the 12th grade, about half of the adolescents have abused an illicit drug like "marijuana" at least once[25]. The other side of the coin makes these drugs in combination with cannabinoids receptor effective against various immune events and plays vital role in pain transmission, and neurodegenerative disorders[26]. The four ligands used in the present study are AM-1221, AM-2232, UR-144, and JWH-015[27, 28, 29, 30]. All these ligands are the agonist and show higher binding affinity towards CB2 than CB1. Among these four ligands, AM-1221 has greater affinity towards CB2 due to presence of 2-methyl and 6-nitro group on the indole ring which makes it's highly CB2 selective. The structures of these ligands along with CB2 receptor are shown in Figure 1,

2. Methods

2.1. Homology Modeling and sequence alignment

The UniProt database(http://www.uniprot.org) were used to retrieve the amino acid sequence of Cannabinoid receptor type 1 and type-2. The sequence are as follows:

CB1 Sequence (UniProt accession code: P21554)

MKSILDGLADTTFRTITTDLLYVGSNDIQYEDIKGDMASKLGYFPQKFPL
TSFRGSPFQEKMTAGDNPQLVPADQVNITEFYNKSLSSFKENEENIQCGE
NFMDIECFMVLNPSQQLAIAVLSLTLGTFTVLENLLVLCVILHSRSLRCRP
SYHFIGSLAVADLLGSVIFVYSFIDFHVFHRKDSRNVFLFKLGGVTASFTA
SVGSLFLTAIDRYISIHRPLAYKRIVTRPKAVVAFCLMWTIAIVIAVLPLLG
WNCEKLQSVCSDIFPHIDETYLMFWIGVTSVLLLFIVYAYMYILWKAHSH
AVRMIQRGTQKSIIIHTSEDGKVQVTRPDQARMDIRLAKTLVLILVVLIIC
WGPLLAIMVYDVFGKMNKLIKTVFAFCSMLCLLNSTVNPIIYALRSKDLR

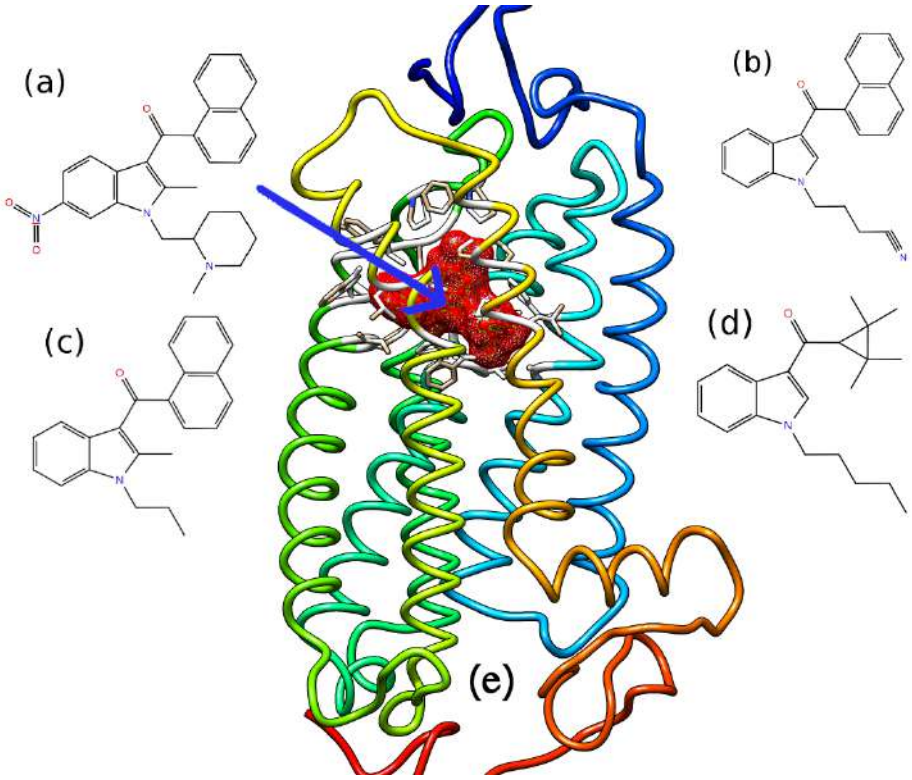

Figure 1: Chemical structures of small-molecule ligands (a) AM-1221, (b) AM-2232, (c) JWH-015, (d) UR-144, respectively. (e) Induced fit docking ligand AM-1221 (red color surface-mesh) into binding pocket of cannabinoid receptor type-2.

HAFRSMFPSCEGTAQPLDNSMGDSDCLHKHANNAASVHRAAESCIKSTV
KIAKVTMSVSTDTSAEAL

CB2 Sequence (UniProt accession code: P34972)
MEECWVTEIANGSKDGLDSNPMKDYMILSGPQKTAVAVLCTLLGLLSAL
ENVAVLYLILSSHLRRKPSYLFIGSLAGADFLASVVFACSFVNFHVFHGVD
SKAVFLLKIGSVTMTFTASVGSLLLTAIDRYLCLRYPPSYKALLTRGRALV
TLGIMWVLSALVSYLPLMGWTCCPRPCSELFPLIPNDYLLSWLLFIAFLF
SGIIYTYGHVLWKAHQHVASLSGHQDRQVPGMARMRLDVRLAKTLGLV
LAVLLICWFPVLALMAHSLATTLSDQVKKAFAFCSMLCLINSMVNPVIYA
LRSGEIRSSAHHCLAHWKKCVRGLGSEAKEEAPRSSVTETEADGKITPW
PDSRDLDLSDC

Due to lack of the experimentally crystallized structure of protein of interest, homology modeling provides a robust path to predict the correct 3D structure of the proteins. Till date there is no experimental crystal structure available for the CB receptor-type 2, and therefore we built homology model for CB2. CB1 and CB2, two subtypes of receptors show nearly 44 % match in the entire protein sequence as well as almost 75 % in the seven trans-membrane regions. This homology modeling begins with templet identification, alignment, model building till refinement. Once the 3D models were build, it will be rigorously validated by investigating the various structural parameters and related structural quality assessment.

We used Prime[31, 32, 33] for the construction of 3D model for protein and refinement followed by their validation using BioLuminate suite[34, 35, 36, 37]. BLAST homology search which fetch the regions of local similarity between biological sequences was adopted to point out the best homologous experimental protein structure from protein data-bank repository[38]. BLOSUM62 similarity matrix was used to calculate the alignment score of sequence alignment. A database protein must have at least 40 % sequence identity, high resolution and the most appropriate cofactors for it to be considered as a template sequence.

We used the gap opening penalty cost of 11.0 for the gap in sequence alignment and there is a 1.0 penalty score for each gap extension. BLAST homology search with an inclusion threshold of 0.005 was accomplished for maximum of three iterations. Once the 3D models were built then it will be rigorously validated by investigating the various structural parameters and related structural quality assessment. We used the thermo-stabilized human A2A receptor (PDB code: 2YDO)[39] as a base templet for the active state of CB2. The crystal structure of the human cannabinoid Receptor CB1 is recently reported[40]. SSPro was used for the prediction of the secondary structure whereas Prime STA GPCR-specific alignment was owned for the sequence alignment. We employed knowledge based model building method to construct 10 models in each run. We also used a VSGB solvation model to refine the loops with OPLS 2005 force field and their respective charges. After construction of the main chain atoms, next target is to assign their position accurately. This is important to figure out protein-ligand interactions at the active sites and the protein-protein interact at their contact interfaces. The in-home build 3D model was then energy minimized to remove the atomic clashes. The final refined model must be evaluated for checking the angles, chirality, bond lengths, close contacts etc. using the BioLuminate suite. One can build a successful model based on correct template selection, algorithm used and the validation of the model.

2.2. Protein preparation

We prepare protein in protein preparation wizard of Schrödinger[41, 42] before kickoff ligand-docking. In protein preparation, the structure is typically imported from Protein Data Bank (PDB) and the unwanted water molecules were removed. In this wizard, the original hydrogen atoms were removed with the new ones and the bond order are adjusted to rectify the errors in the proteins. Structures with missing residues near the active site must get repaired. By adjusting the orientations and relative state of the interacting groups like ASN, GLN, TYR, THR, SER, and HIS, hydrogen bonding network were corrected. At last, the protein structure was then refined by restrained energy minimiza-

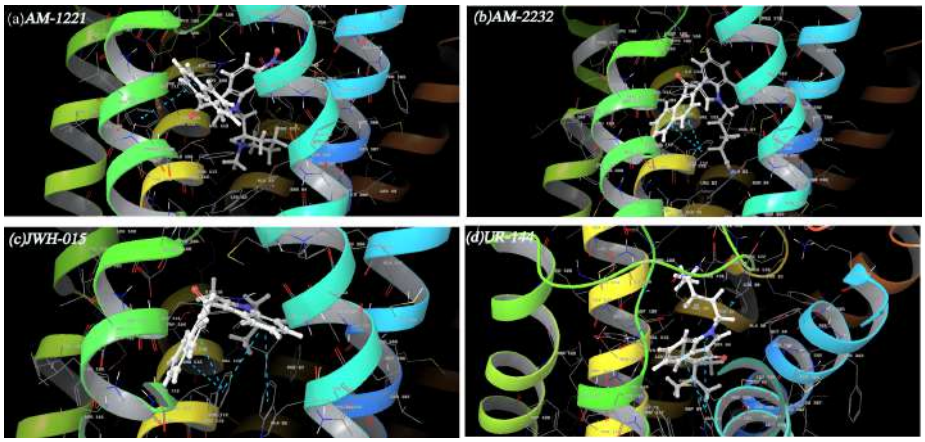

Figure 2: The 3D structure of ligands (a) AM-1221, (b) AM-2232, (c) JWH015, and (d) UR-144 inside the binding pocket of the cannabinoids receptor type 2. The pi-pi interaction between the ligand and residues of CB2 receptor is shown in cyan dashed line.

tion by employing OPLS 2005 force field. The structure of the cannabinoids receptor type 2 with ligand AM-1221 after docking is shown in Figure 1(e).The crystal structure of CB1 (PDB accession code: 5XR8) was used as the template structure for modeling studies of CB1[40] .

2.3. Ligand preparation

Appropriate preparation of ligand structures is necessary for the modeling/docking task. This can be achieved by LigPrep[43] module of Schrödinger to prepare the 3D ligands. Maestro 2D sketcher is used to prepare the initial ligands structure and further converted into 3D structures to produce corresponding low energy 3D output. We are not performing any pre-docking filtering and included all the structures. We prepared ligands with the OPLS 2005 force field and charges and we only conserve those ligands which have low energy conformers.

2.4. Induced fit docking (IFD)

The receptors are not rigid in nature whereas the standard virtual docking studies assume it as a rigid receptor. To overcome this issue, we perform the Induced fit docking method by using the Induced fit Docking (IFD) protocol[44, 45] of Schrödinger for ligand docking to predict their binding mode and impact on structural changes of the receptor. We prepared a docking receptor grid using cavities that are stuffed by THR97, PHE100, TRP179, THR183, and MET263 for Cannabinoids receptor type-1 and PHE87, THR116, PHE117, ILE198 and TRP258 for Cannabinoids receptor type-2 [46]. Constrained minimization of the receptor has been performed with an RMSD cutoff of 0.18 Åusing a softened potential glide docking was performed for each ligand. A maximum of 20 poses for each ligand are retained and these poses must satisfy the criteria of Coulomb-vdW score below 100 and the H-bond score less than 0.05. To make best protein/ligand flexible binding domain, Prime Molecular Dynamics module was used and applied to those amino residues which fall with-in 5 Åof each pose. Glide re-docking of each set of protein/ligand complex were performed using GlideSP[47] with the best 20 poses within 30 kcal/mol.

2.5. Molecular dynamics simulations

The coordinates of the best result from the CB1 and CB2 docking poses were undergoes through molecular dynamics simulation by DESMOND software[48, 49, 50, 51] using OPLS2005 force field. To setup the system, we used the system builder module of the DESMOND and immersed the complex into the POPC membrane with neutralizing counter ions with per-equilibrated TIP3P water bath at 303 K such that the prepared system was surrounded by a periodic box of waters and is extended approximately 10 Åin each direction. The RESPA integrator algorithm [52] was employed in the numerical integration with a bonded time step of 2ps. Nose-Hoover Chain[53] thermostat method has used to control the thermostat with a relaxation time step of 1.0 ps. Barostat method proposed by Myntra-Tobias-Klein[54] was employed with a relaxation time step of 2.0ps

Table 1: The details of protein family and the globally conserved residue for CB2 receptor.

Query	Templet: PDB ID	% Identity	% Similarity	Family	E-value
CB2	2YDO	26	46	7TM_1- 7 Transmembrane Receptor (Rhodopsin Family)	1.2e-44

with isotropic-molecule-based scaling to maintain the constant pressure during simulation. For Lennard-Jones interactions, a cutoff of 9.0 Åwas applied for the short range coulombic interactions and smooth particle mesh Ewald method was used with tolerance of 1e-09 for long range forces. The generated system is then energy minimized for 5000 iterations. After the minimization of the structure, the system undergoes six relaxation steps before the molecular dynamics production step begins. After initial equilibration, the 100ns production trajectories are generated using NPT ensemble for various structural and dynamical analysis. RMSD, RMSF and other structural feature are computed using inbuilt simulation interaction method of DESMOND.

3. Results and discussion

Homology modeling administer unique and transparent way to generate 3D model of proteins having significant importance in science/nature because of large ratio between the number of known protein sequence and number of solved proteins structure[55]. In our study, we prepared ten 3D models of Cannabinoids receptor type 2 (CB2) and conserved the best residue for our docking and simulations. It is recommended to check the structural closeness in the protein family and general behavior in their structural and biological properties. The details of protein family and the globally conserved residue is given in table 1. By defining the class of family and globally conserved residues, one gets the precise idea about the experimental 3D feature of the protein of interest. We used the templet with highest matching sequence identity with our target sequence. Induced Fit Docking (IFD) module of Schrödinger was used for the docking of the ligands in cannabinoids receptors. We performed this module explicitly over other docking modules because in IFD, ligands induce the conformational

changes in the active site of protein upon binding. Standard docking module such as SP and XP, assumes that receptors are rigid in nature but it's not the case as receptor/protein shows flexible behavior in their shape and binding modes while interacting with ligands.

3.1. Docking Results

The docking results for all the four ligands into the CB2 receptor are shown in Figure 2. In this figure the docking/binding site are zoomed in order to explore the type the interaction ligands makes with surrounding residue of CB2. In the Induced Fit Docking (IFD) of ligand AM-1221 into CB1 and CB2 receptor shows docking score of -13.48 and -12.729 kcal/mol, respectively. For the case of CB1 (Figure 3a), the residue THR201 shows direct side chain hydrogen bonding with the ligand inside the binding pocket and makes it stable. The residues VAL291, PHE278, ILE290, TRP279, LEU360, LEU359, MET363, ILE362, PHE379, PHE177, CYS382, CYS386, LEU387, VAL 96 and PHE174 shows hydrophobic interaction with the AM-1221 ligand inside the pocket with in the 4Åcut off. The residues THR197, SER199, SER 383 and SER390 also shows polar interaction with the ligand. The pi-cation interaction is also found between the ligand and the residues PHE200 and PHE170.

For IFD of ligand AM-1221 in CB2 receptor, the residue VAL113 shows direct hydrogen bonding with the ligand which makes its stable in binding pocket. Other residues like PHE 197 and PHE 87 shows $\pi - \pi$ interaction and $\pi - \pi$ stacking respectively. The ligand experiences hydrophobic interaction with the nearby residue like ALA83, PHE117, PRO 178, TYR 190, LEU 191, TRP 194, ILE 198 with in the 4 Åcut off as shown in Figure 4a. The residue ASP189 shows positive charged interaction towards ligand. The ligand shows polar interaction by THR114, THR116, ASN188, SER 193 and SER285 with in the same range of cutoff. The ligand interaction diagram describes the various interaction shown in Figure 3 and 4.

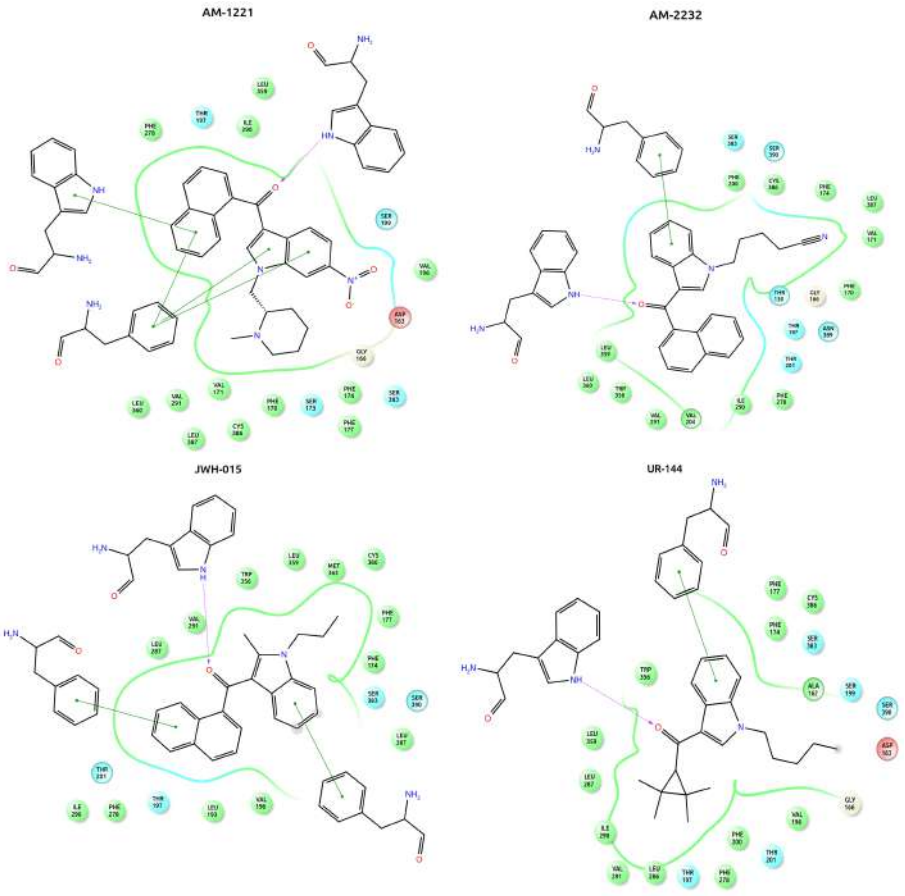

Figure 3: The ligand interaction diagram of (a) AM-1221, (b) AM-2232, (c) JWH-015, (d) UR-144, respectively with cannabinoids receptor type 1. The hydrophobic interaction within 4 Å region of ligand with resides are shown in green color whereas the $\pi - \pi$ interaction is demonstrated by green solid line.

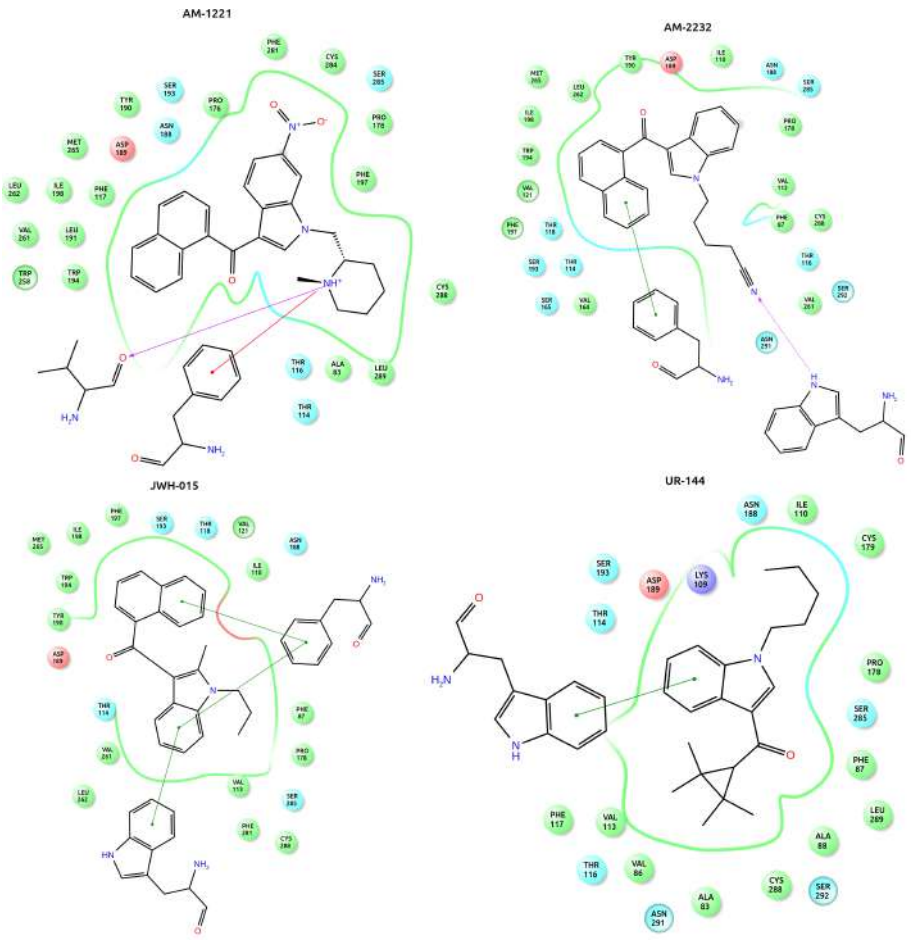

Figure 4: The ligand interaction diagram of (a) AM-1221, (b) AM-2232, (c) JWH-015, (d) UR-144, respectively with cannabinoids receptor type 2. The hydrophobic interaction within 4 Å region of ligand with resides are shown in green color whereas the $\pi - \pi$ interaction is demonstrated by green solid line.

We performed the similar docking protocol for the AM-2232 ligand in the CB1 and CB2 receptor. The docking score is found to be -12.38 and -11.048 kcal/mol, respectively. The residue TRP279 makes direct hydrogen bonding with the ligand inside the binding pocket with the oxygen atom. The residues PHE278, ILE290, VAL204, VAL291, TRP356, LEU360, LEU359, CYS386, PHE200, PHE170, PHE174, LEU387, and VAL171 shows hydrophobic interaction with the ligand within the 4 Åcut off as shown in Figure 3b. Residues like SER383, ASN389, THR201, THR197, THR130 and SER390 influences the polar interaction with the ligand. The residue PHE177 shows $\pi - \pi$ stacking with the ligand inside the binding pocket of CB1 receptor.

This ligand also shows the affinity towards the CB2 receptor with greater extent. In Figure 4b, the Residue TRP258 shows direct hydrogen bonding with the terminal Nitrogen atom of the ligand and PHE117 shows the $\pi - \pi$ stacking with the nearby two rings of the ligand with equal strength. In the binding capsule, the ligand is well trapped with the residues like PHE87, VAL121, PRO178, TYR190, TRP194, ILE198, LEU262, MET265 with the hydrophobic interaction within 4Åregion. Some polar residues like THR114, THR116, THR118, ASN 188, SER 165, SER 286 also shows interest in stabilizing the ligand in the pocket. The ligand is also approached by the negatively charged moiety ASP189. In literature and experimentally offered results also confirms the same behavior of the ligand with receptor[56, 57].

Another agonist subtype-selective cannabinoid ligand of interest is JWH-015. Like other two, it also shows deep interest and stability in the binding pocket of the CB2. The docking score of this ligand in CB1 and CB2 pocket is -11.86 and -10.745 kcal/mol, respectively. For CB1-JWH-015 system, the docked ligand shows direct hydrogen bonding interaction with the TRP279 residue of receptor as shown in Figure 3c. Whereas the residues like ILE290, PHE278, LEU287, VAL291, MET363, TRP356, LEU359, CYS386, PHE174, PHE177, LEU387, VAL196, LEU193 shows hydrophobic interaction with the docked ligand. Few residues like SER390, THR197, THR201 AND SER383 shows polar interaction with the ligand. The residue PHE170 shows the $\pi - \pi$ stacking with the docked

ligand.

Figure 4c shows that CB2 protein does not shows any direct hydrogen bonding feature with the polar groups of ligands, but its shows $\pi - \pi$ stacking with PHE117 and TRP258 residues. There is a list of residues shows hydrophobic interaction with JWH-015 and is tier as PHE87, VAL113, ILE110, MET265, VAL121, TYR190. Residue ASP189 also shows negatively charged interaction towards the ligand. This ligand is also stabilized by the polar group present in the binding pocket by residues lined as SER193, THR118, THR114, ASN188, SER285 within the cutoff range of 4Å. This ligand binds CB2 receptor roughly 30 times more strongly when compared with the CB1[58]. Finally, the synthetic drug we docked in the cannabinoid receptors is UR-114. This ligand also shows interactive behavior and get stabilized when perfectly docked in the binding pocket of the CB1 and CB2 receptor. The docking score shows a value of -10.63 and -9.384 Kcal/mol for CB1 and CB2, respectively. This reduction is docking score compared with earlier three ligands is due to the structure of drug as it contains substituted cyclo-propane ring. In CB1 (Figure 3d), this ligand shows direct hydrogen bond interaction with the side chain of the TRP279 residue of receptor. The ligand experiences hydrophobic interactions with the PHE278, ILE290, LEU286, PHE200, PHE174, PHE177, CYS386, VAL196, ALA162, and VAL291 residues. There is also a charged interaction between ligand and ASP163 residue. The $\pi - \pi$ stacking is shown by residue PHE170 with the docked ligand. The residues THR197, THR201, SER199 and SER383 shows polar interaction with the docked ligand. It shows higher affinity towards the CB2 but behaves roughly 85 times weaker affinity towards CB2[59]. Figure 4d display that, UR-144 ligand shows only $\pi - \pi$ interaction with the nearby residues like PHE87 and TRP 258. There is signature of hydrophobic interaction with the surrounding residues like ILE 110, PRO, 178, PHE87, ALA88, PHE117, VAL113, VAL86. This ligand also shows polar residues interaction with THR114, THR116 SER285, ASN188 within the range of 4Å. Negatively and positively charged residues like ASP189 and LYS109 also plays key role in stabilizing this ligand into the binding pocket of CB2 receptor.

Table 2: The induced fit docking (IFD) results (kcal/mol) and glide emodel of the four ligands with cannabinoids receptor type 1 and type 2.

Ligands	Docking Score (kcal/mol)		Glide E-model	
	CB1	CB2	CB1	CB2
AM-1221	-13.48	-12.73	-112.02	-102.36
AM-2232	-12.38	-11.05	-101.22	-91.37
JWH-015	-11.86	-10.75	-89.35	-80.61
UR-144	-10.63	-09.38	-77.21	-66.10

The docking results and glide emodel are tabulated in Table 2. To strengthen our results from Induced fit docking, we also performed the molecular dynamics simulation using DESMOND[50] discussed in next subsection.

3.2. Simulation results

We performed MD simulations using DESMOND module of Schrödinger which initiate with the best docked ligand into protein. The stability of the docked ligand inside the protein has been verified by the simulation. We computed the protein-ligand Root Mean Square of Deviation (RMSD) to measure the average fluctuation in the selection of atoms for a frame with respect to first frame (reference frame).

The RMSD can be formulated for frame x is:

$$RMSD_x = \sqrt{\frac{1}{N}\sum_{i=1}^{N}(r_i(t_x)) - r_i(t_{ref}))^2} \tag{1}$$

Where N is the number of chosen atoms, t_{ref} is correspond to reference time and generally set to 0 for first frame, r_i is the position of the selected atoms belong to the frame x recorded at time t_x. To calculated RMSD this procedure is repeated for every frame along the simulation trajectory.

The Figure 5 shows the protein-ligand RMSD for all the four ligands with CB1 and CB2 receptor, respectively. Walking along the x-axis gives you indication

about the stability of ligand with respect to the protein in its binding pocket. This plot 5 shows that the ligand which bind to protein firstly align along the protein backbone of the reference and then remain there for rest of the time. Here we present the results based on 100ns simulation trajectory and probably this simulation length is good enough to explain the stability of ligand inside the binding pocket of protein. We can also conclude from the plot 5 that the observed values for ligands are lower than that of protein that makes ligand stable inside the pocket otherwise in reverse condition the ligand will diffuse away from its initial binding site. For AM-1221 with CB1 and CB2 (Figure 5a and 5b), the average fluctuation in RMSD of protein and ligand is averaged between 4.0-5.0 Åand 2.6-3.6 Årespectively. Fluctuation falls within the range of 1-3 Åare acceptable for considerable number of small and globular proteins. The above results show that our simulation is well converged and fluctuating along average value for both protein and ligands. The results of protein ligand RMSD for ligand AM-2232 with CB1 and CB2 are shown in Figure 5c and 5d demonstrate the well converged structure of ligand inside the binding pocket of protein docked initially along the 100ns simulation trajectory. The average fluctuation of protein and ligand are 4.25-4.75 Åand 1.0-2.0 Årespectively. The overall simulation results show that ligand is stable at the same place where it was initially docked in the beginning of the simulations. We also looked for the protein-ligand RMSD data for the ligand JWH-015 and UR-144. The Figure 5e,5f and 5g,5h represent the ligand-protein RMSD plot of JWH-015 and UR-144 into CB1 and CB2, respectively. Here we also got the similar trend in the behavior of deviation as we got for other two cases. The average fluctuation of protein and ligand is 4.0-5.0 Åand 4.6.-5.6 Åfor UR-144. Similarly, the average fluctuation of protein and ligand is 4.0-5.0 Åand 2.7-4.2 Åfor JWH015.

Another important property that deals with the structural stability of protein is Root Mean Square Fluctuation (RMSF). This RMSF is useful in characterizing the local structure changes that occur during simulation along the protein. It

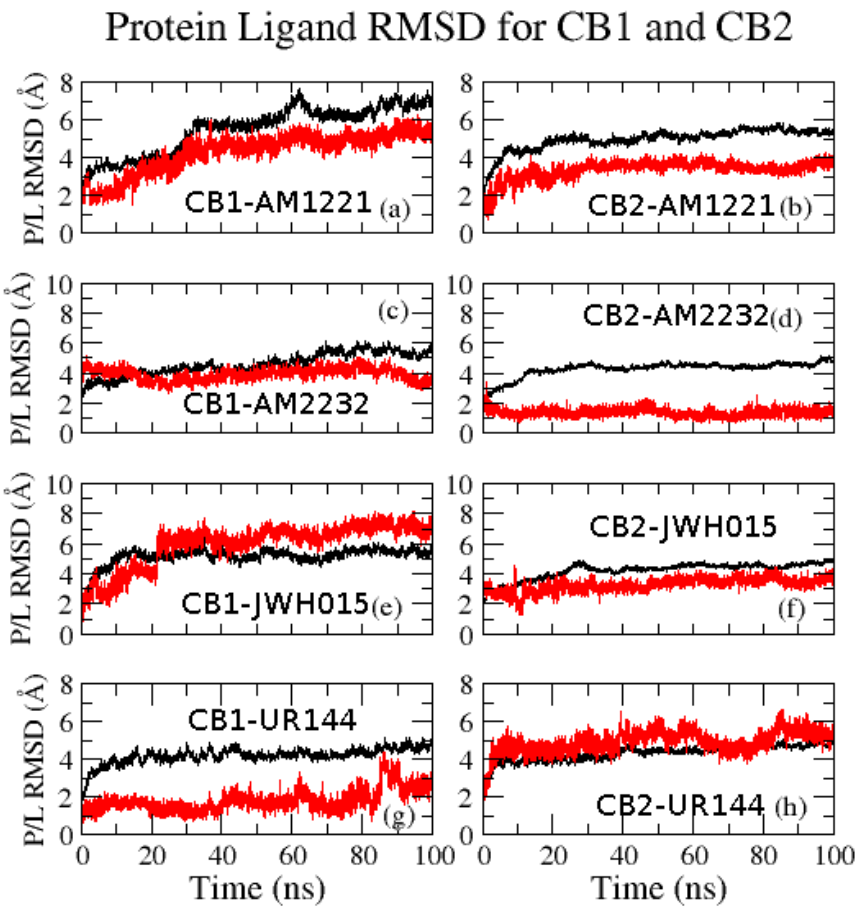

Figure 5: The protein-ligand root mean square deviation (RMSD) for ligands (a) AM-1221,(c) AM-2232, (e) JWH-015, and (g) UR-144 with CB1 and RMSD of ligands (b) AM-1221,(d) AM-2232, (f)JWH-015, and (h) UR-144 with CB2. The black curve denoted protein where as the red curves displays ligand RMSD, respectively.

is formulated as,

$$RMSF_i = \sqrt{\frac{1}{T}\sum_{t=1}^{T}\langle(r_i(t)) - r_i(t_{ref}))^2\rangle} \tag{2}$$

Where, t is termed as trajectory time over which RMSF is calculated, reference time is denoted by t_{ref}, r_i is position of residue I, and angular bracket denotes the average over the selection of atoms in the residue.

In RMSF plot, the peak indicates those proteins that fluctuate during the simulations. Lower fluctuation can be directly correlate with the ligand binding site inside the binding pocket. From Figure 6(a,b) we see that the tails of the protein fluctuate more than any other part of the proteins (CB1 and CB2). Usually rigid elements like alpha helix and beta strands fluctuates less as they are more structured compared with the loop regions. The ligand which is interacting with the protein make it stable and not allowed it to fluctuate much when compared with the free moiety. We can also explain the fluctuation based on ligands fluctuation by Ligand Root Mean Square Fluctuation (RMSF). This is formulated in the comparable way as protein RMSF. This is also an important quantity which will give the clear view how individual ligand fragment interact with the receptor protein. This fluctuation shows the entropic role of binding between ligand and receptor. This function comes into play once the protein-ligand complex aligned on the protein backbone and then ligand RMSF is measured on the ligand heavy atoms (Figure not shown). We found that ligand AM-1221 and AM-2232 are more flexible when compared with the UR-144 and JWH-015. This leads to their way of interaction inside the binding pocket of receptor. The ligand AM-1221 interact with more strength with the CB2 receptor and show greater stability over the other ligands. This can also be explained based on their CB2 activity and corresponding docking scores.

Furthermore, the contacts between ligand and protein will be more specifically explored on the basis of their interaction or contacts. These interactions are mobile and fluctuates during simulations. Moreover, these interactions are subdivided into four categories namely: Hydrogen bond, Hydrophobic, Ionic

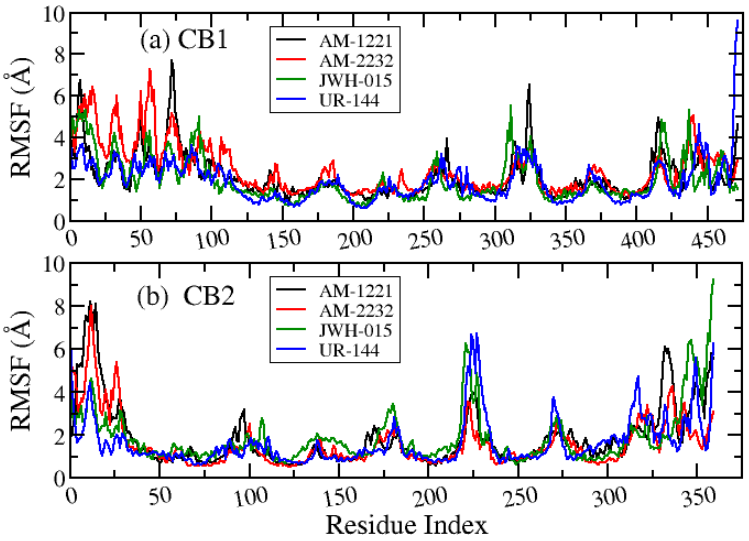

Figure 6: The protein-ligand root mean square fluctuation (RMSF) of AM-1221, AM-2232, JWH-015, and UR-144 with cannabinoids receptor (a) type 1 and (2) type 2, respectively.

and water bridge. Hydrogen bonding properties plays a significant role in drug design as it influences a strong impact on drug specificity, metabolization and adsorption. The geometric criteria for protein ligand hydrogen bond is set to be distance of 2.5 Åbetween donor and acceptor atoms (D-H—A). A donor angle of $\geq 120^{\circ}$ between the donor-hydrogen-acceptor atoms (D-H$\cdots$A); and an acceptor angle of $\geq 90^{\circ}$ between the hydrogen-acceptor-bonded atom atoms (H$\cdots$A-X). Hydrogen bonding is further sub-categorized into backbone acceptor; backbone donor; side-chain acceptor; side-chain donor. The ligand experienced hydrophobic interaction with near-by protein residues mainly by π-cation, $\pi - \pi$ stacking or due to other interaction. The geometric criteria for hydrophobic interaction for π-Cation-Aromatic and charged groups falls within 4.5 Å; for $\pi - \pi$ interaction, two aromatic groups must be stacked face-to-face or face-to-edge. Other interaction is just an on-specific hydrophobic side chain within 3.6 Åof a ligands aromatic or aliphatic carbons. The Figure 7 shows the Interaction diagram of the ligands with CB2 along the simulation trajectory. For ligand AM-1221 in CB2, ASN188 makes H-bond through side chain with 7.0% probability. Residues like ALA83, PHE87, PHE94, VAL113, PHE117, PRO178, TRP258, VAL261, MET265, PHE281, CYS288 and LEU289 shows hydrophobic interaction with strength ranges from 5% to 75%. Residues (% strength) like PHE281 (32%), TRP258 (4%), PHE97(7%), PHE94(7%), PHE91(12%) shows profound $\pi - \pi$ stacking. LYC103 (4%) and PHE117 (2%) shows some signature of π-cation interaction. LYC103 also involved in the ionic interaction with ligand. Water molecules present in the system makes "bridge" between ligand and amino acids either through donor or acceptor mechanism. THR114, VAL164, SER193 act as hydrogen bond acceptor while LYS103 acts as hydrogen bond donor. Some amino acid like ASN188 and ASP189 categorized as both acceptor and donor moiety. For the case of AM-2232 ligand, the amino acid ASN188 makes H-bond through side chain with 9.0% probability. Amino acids PHE87, ILE110, VAL113, PHE117, TYR190, TRP 194, ILE198, VAL261, MET265, CYS288 shows hydrophobic interaction and amino acids (% strength) like PHE87 (44%), PHE117(37%) and TYR190 (6%) involved in the $\pi - \pi$ stacking with ligand.

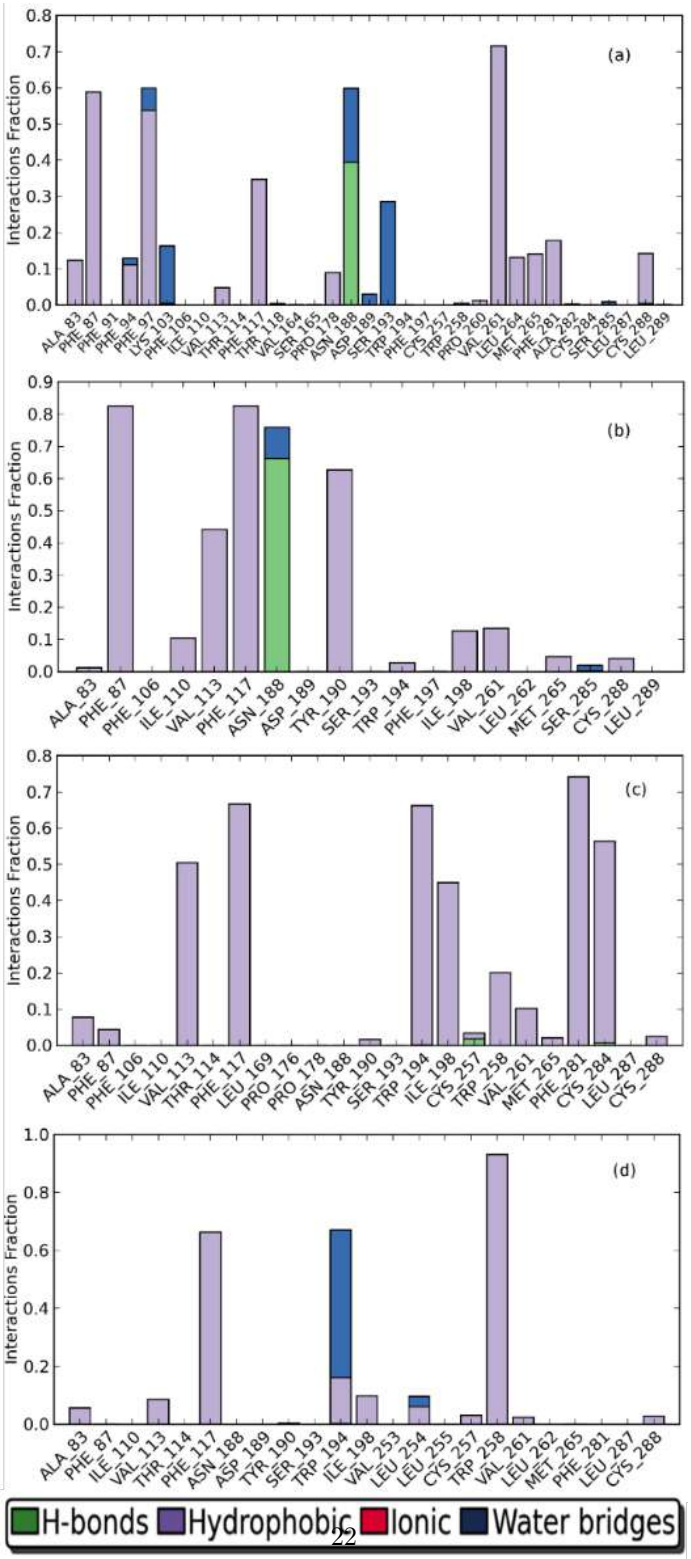

Figure 7: Interaction diagram of CB2 with compounds (a)AM-1221, (b) AM-2232, (c) JWH-015, (d) UR-144.

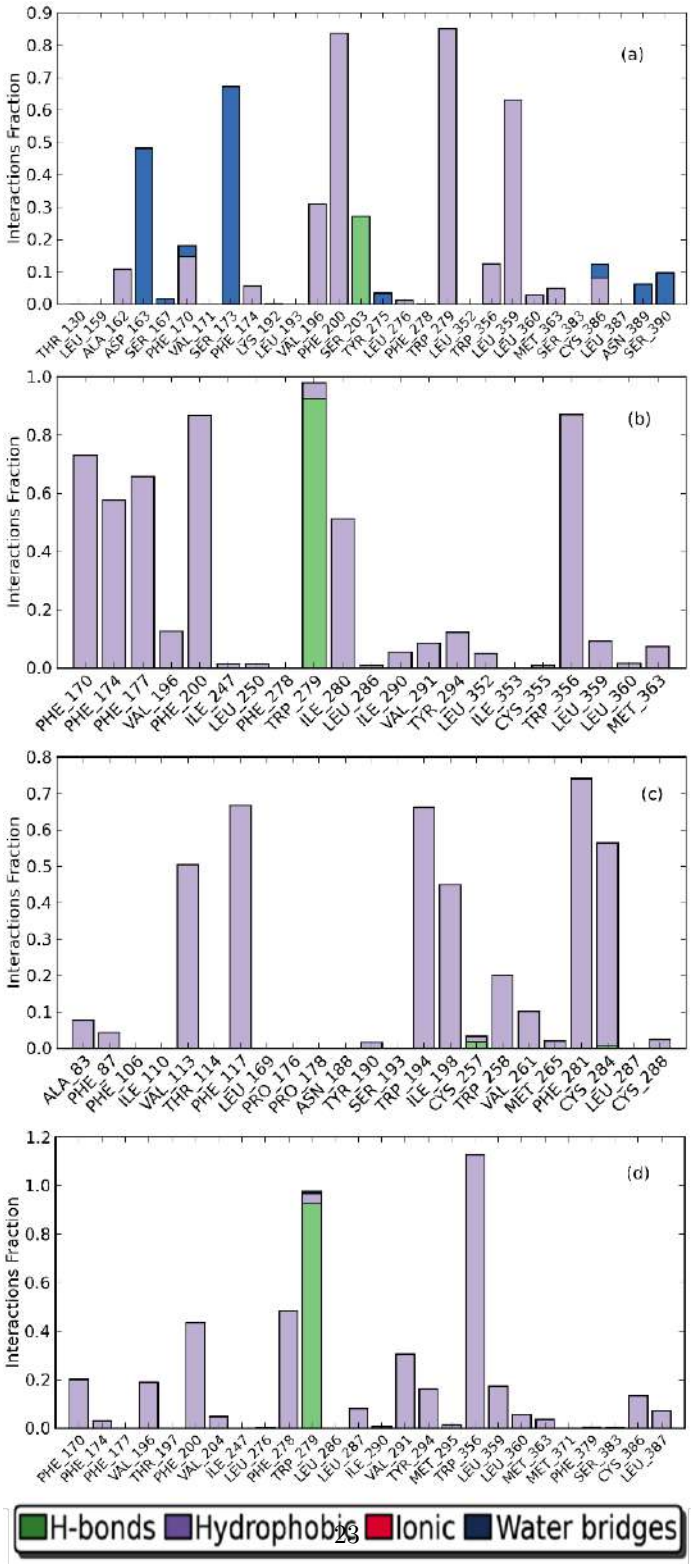

Figure 8: Interaction diagram of CB1 with compounds (a)AM-1221, (b) AM-2232, (c) JWH-015, (d) UR-144.

No ionic interaction is detected throughout the simulation. The acceptor type water bridge between amino acid ASN188, SER193 and SER285 with ligand. Only residue ASN188 shows donor behavior. For the case of ligand JWH-015, the amino acid THR114, TRP194, CYS284 makes weak side chain hydrogen bond of strength less than 2%. Hydrophobic interaction leads by the several amino acid residues like PHE87, ILE110, VAL113, PHE117, TRP194, ILE198, TRP258, VAL261, PHE281, CYS284. Residues PHE87, PHE117, TRP194, TRP258, PHE281 shows $\pi - \pi$ stacking with strength 2% to 37%. No ionic or water bridge contact between ligand and amino acid residues. Amino acid THR114 makes side chain hydrogen bond with the ligand UR-144 with 21% in strength. The interaction types and fractions are shown for the interacting amino acids throughout the course of MD simulations. Residues like ALA83 PHE87, VAL113, PHE117, TRP194, ILE198, TRP258 shows hydrophobic contact whereas the residues PHE117 and TRP258 shows $\pi - \pi$ stacking with percentage strength of 18% and 54% respectively. No ionic interaction reported in this case. Few residues like ASN188, ASP189, LEU254 perform acceptor behavior in water bridge whereas THR114 and TRP194 deals with the donor behavior. In present work, we restrict our explanation only for CB2 results although the protein-ligand RMSD for all the four ligands with CB1 are shown in Figure 8.

The stability of ligands inside the protein binding pocket can also be explained based on the interaction energy between ligand and protein. The potential energy of the system (protein+ ligand + water) is given by

$$E_{total} = E_{Col} + E_{vdW} + E_{bond} + E_{angle} + E_{torsion} \tag{3}$$

Electrostatic interactions mainly classified into charge-charge, charge-dipole, and dipole-dipole interaction between ligand-protein binding site. The charge-charge interactions arise in between oppositely positively or negatively charged atoms, ligand functional groups, or protein side chains. The interactions between ionized amino acid side chains and the dipole of the ligand moiety also

contribute towards the enthalpy change associate with binding due to charge-dipole interaction. Dipole moment from the polar side chain of amino acids influence the ligand-protein interaction. Binding event also influenced by the Van der Waals interaction and is important quantity to elucidate the structure and interaction of biological species. We used the simulation event analysis tool from DESMOND to estimate the binding energy due to the non-bonded interaction between a ligand and a binding site of protein. Based on the calculated binding energy, ligand AM-1221 shows total interaction energy of -58.64 kcal/mol which makes it quite stable in the pocket. Other ligands AM-2232, UR-144 and JWH-015 shows binding energy of -55.77, -48.53, and -48.25 kcal/mol respectively.

Conclusions

We used multiple template comparative homology modeling algorithms to construct 3D model for CB2. We performed docking and molecular dynamics simulation study of four synthetic drugs in both the CB1 and CB2 receptors. Our docking and simulation results show a better affinity of the ligands towards cannabinoid receptors, and they are reasonably stable inside the binding pocket. The ligand AM-1221 shows the highest binding affinity -12.73 Kcal/mol, whereas UR-144 shows the lowest -9.83 Kcal/mole towards CB2 receptor. Molecular properties of the ligands, including molecular, polar, and solvent accessible surface areas, and intra-molecular hydrogen bonds were evaluated throughout the course of molecular dynamics simulations also supports the agonist activity of ligands towards cannabinoids receptor-2. The computed results should engross the design of ligands with distinct pharmacological properties associated with cannabinoid receptor type-2.

4. Acknowledgments

V.K.Y. gratefully acknowledges the Science and Engineering Research Board (SERB), Department of Science and Technology (DST), Government of India for the National Post-Doctoral Fellowship (Grant PDF/2019/001240). V.K.Y. also like to thank Dr. Khaled. M. Elokely for helping in the initial setup of the systems. I also want to pay sincere thanks to Prof. Michael L. Klein for the valuable discussion. Part of the calculations was carried out at the High-Performance Computing Facility (OwlsNest) of Temple University, Philadelphia, U.S.A.

5. ORCID

http://orcid.org/0000-0002-9142-4567

References

[1] Edery, H., Grunfeld, Y., Ben-Zvi, Z., Mechoulam, R., Structural requirements for cannabinoid activity. Ann. N.Y. Acad. Sci., 1971, **191**, 40-53.

[2] Gaoni, Y., Mechoulam, R. Isolation, structure and partial synthesis of an active constituent of hashish. J. Am. Chem. Soc., 1964, **86**, 1646-1647.

[3] Martin, B.R., Balster, R.L., Razdan, R.K., Harris, L.S., Dewey, W.L. Behavioral comparisons of the stereoisomers of tetrahydrocannabinols. Life Sci., 1981, **29**, 565-574.

[4] Lambert, D.M., Fowler, C.J., 2005. The Endocannabinoid System: Drug Targets, Lead Compounds, and Potential Therapeutic Applications. Journal of Medicinal Chem., 2005, **48(16)**, 5059-87.

[5] Pertwee, R., ed. Cannabinoids. Springer-Verlag. 2005, p. 2.

[6] Galiegue, S., Mary, S., Marchand, J., et. al. Expression of central and peripheral cannabinoid receptors in human immune tissues and leukocyte subpopulations. European Journal of Biochemistry, 1995, **232 (1)**, 54-61.

[7] Hanson, M.A., Roth, C.B., Jo, E., et. al. Crystal structure of a lipid G protein-coupled receptor. Science, 2012, **335**, 851-855.

[8] Wu, H., Wacker, D., Mileni, M., et. al. Structure of the human-opioid receptor in complex with JDTic. Nature 2012, **485**, 327-332.

[9] Manglik, A., Kruse, A. C., Kobilka, T. S., et. al. Crystal structure of the micro-opioid receptor bound to a morphinan antagonist. Nature, 2012, **485**, 321-326.

[10] Wang, C., Jiang, Y., Ma, J., et. al. Structural basis for molecular recognition at serotonin receptors. Science 2013, **340**, 610-614.

[11] Pacher, P., Mechoulam, R., Is lipid signaling through cannabinoid 2 receptors part of a protective system?. Progress in Lipid Research, 2011, **50(2)**, 193-211.

[12] Ashton, J.C., Wright, J.L., McPartland, J.M., et. al., Cannabinoid CB1 and CB2 receptor ligand specificity and the development of CB2-selective agonist. Curr. Med. Chem, 2008, **15**, 1428-1443.

[13] Huffman, J.W., Marriott, K.S.C., Recent advances in the development of selective ligands for the cannabinoid CB2 receptor. Curr Top Med. Chem, 2008, **8**, 187-204.

[14] Benito, C., Nunez, E., Tolon, R.M., et al. Cannabinoid CB2 receptors and fatty acid amide hydrolase are selectively overexpressed in neuritic plaque-associated glia in Alzheimer's disease brains. The Journal of Neuroscience, 2003, **23 (35)**, 11136-11141.

[15] Fernandez-Ruiz, J., Pazos, M.R., García-Arencibia, M., Sagredo, O., Ramos, J.A., Role of CB2 receptors in neuroprotective effects of cannabinoids. Molecular and Cellular Endocrinology, 2008, **286**, S91–96.

[16] Tolon, R.M., Nunez, E., Pazos, M.R., et. al. The activation of cannabinoid CB2 receptors stimulates in situ and in vitro beta-amyloid removal by human macrophages. Brain Research, 2009, **1283 (11)**, 148-154.

[17] Tabrizi, M.A., Baraldi, P.G., Borea, P.A., Varani, K., Medicinal Chemistry, Pharmacology, and Potential Therapeutic Benefits of Cannabinoid CB2 Receptor Agonist, Chem. Rev., 2016, **116**, 519-560.

[18] Baraldi, P.G., Saponaro, G., Moorman, A.R., et. al. 7-Oxo-[1,4]oxazino[2,3,4-Ij]quinoline-6-Carboxamides as Selective CB(2) Cannabinoid Receptor Ligands: Structural Investigations around a Novel Class of Full Agonists. J. Med. Chem., 2012, **55(14)**, 6608-6623.

[19] Aghazadeh, T.M., Baraldi, P.G., Saponaro, G., et. al. Design, Synthesis, and Pharmacological Properties of New Heteroarylpyridine/heteroarylpyrimidine Derivatives as CB(2)Cannabinoid Receptor Partial Agonists. J. Med. Chem., 2013, **56 (3)**, 1098-1112.

[20] Aghazadeh, T.M., Baraldi, P.G., Saponaro, G., et. al. Discovery of 7-oxopyrazolo[1,5-A]pyrimidine-6- Carboxamides as Potent and Selective CB(2) Cannabinoid Receptor Inverse Agonists. J. Med. Chem., 2013, **56(11)**, 4482-4496.

[21] Ibrahim, M.M., Deng, H., Zvonok, A., et. al. Activation of CB2 cannabinoid receptors by AM1241 inhibits experimental neuropathic pain: pain inhibition by receptors not present in the CNS. Proc. Natl. Acad. Sci. USA, 2003, **100**, 10529-10533.

[22] Valenzano, K.J., Tafessem, L., Lee, G., et. al. Pharmacological and pharmacokinetic characterization of the cannabinoid receptor 2 agonist, GW405833, utilizing rodent models of acute and chronic pain, anxiety, ataxia and catalepsy. Neuropharmacology, 2005 **48**, 658-672.

[23] Rice, A.S., Farquhar-Smith, W.P., Nagy, I., Endocannabinoids and pain: spinal and peripheral analgesia in inflammation and neuropathy. Prostaglandins Leukot. Essent. Fatty Acids, 2002, **66**, 243-256.

[24] Richardson, J.D., Aanonsen, L., Hargreaves, K.M. Antihyperalgesic effects of spinal cannabinoids. Eur. J. Pharmacol., 1998, **345**, 145-153.

[25] http://www.hhs.gov/ash/oah/adolescent-health-topics/substance-abuse/illicit-and-non-drug-use.html

[26] Fernandez-Ruiz, J., Pazos, M.R., García-Arencibia, M., Sagredo, O., Ramos, J.A. Role of CB2 receptor in neuroprotective effects of cannabinoids. Molecular and Cellular Endocrinology, 2008, **286**, S91.

[27] Makriyannis, A., Deng, H., Cannabimimetic indole derivatives, granted 2001-06-07.

[28] Makriyannis, A., Deng, H., Cannabimimetic indole derivatives, granted 2007-07-10.

[29] Murataeva, N., Mackie, K., Straiker, A., The CB2-preferring agonist JWH-015 also potently and efficaciously activates CB1 in autaptic hippocampal neurons. Pharmacol. Res., 2012, **66 (5)**, 437-42.

[30] Poso, A., Huffman, J.W. Targeting the cannabinoid CB2 receptor: modelling and structural determinants of CB2 selective ligands. Br. J. Pharmacol, 2008, **153 (2)**, 335-346.

[31] Jacobson, M.P., Pincus, D.L., Rapp, C.S., et. al. A hierarchical approach to all-atom protein loop prediction. Proteins: Structure, Function, and Bioinformatics, 2004, **55**, 351-367.

[32] Jacobson, M. P., Friesner, R. A., Xiang, Z., Honig, B. On the role of the crystal environment in determining protein side-chain conformations. Journal of molecular biology, 2002, **320**, 597-608.

[33] Schrödinger Release 2015-3: Prime, version 4.1, Schrödinger, LLC, New York, NY, 2015.

[34] Zhu, K., Day, T., Warshaviak, D., et. al. Antibody structure determination using a combination of homology modeling, energy-based refinement, and loop prediction. Proteins: Structure, Function, and Bioinformatics, 2014, **82**, 1646-1655.

[35] Salam, N.K., Adzhigirey, M., Sherman, W., Pearlman, D. A. Structure-based approach to the prediction of disulfide bonds in proteins. Protein Engineering Design and Selection, 2014, **27**, 365-374.

[36] Beard, H., Cholleti, A., Pearlman, D., Sherman, W., Loving, K. A. Applying physics-based scoring to calculate free energies of binding for single amino acid mutations in protein-protein complexes. PloS one, 2013, **8**, e82849.

[37] Biologics Suite 2015-3: BioLuminate, version 2.0, Schrödinger, LLC, New York, NY, 2015.

[38] Protein Data Bank (PDB) repository; http://www.rcsb.org

[39] Warne, T., Moukhametzianov, R., Baker, J. G., et. al. The structural basis for agonist and partial agonist action on a [bgr] 1-adrenergic receptor. Nature, 2011, **469**, 241-244.

[40] Hua, T., Vemuri, K., Pu, M., et al. Crystal structure of the human cannabinoid receptor CB1. Cell 2016, **167**, 750–762.

[41] Sastry, G. M., Adzhigirey, M., Day, T., et. al. Protein and ligand preparation: parameters, protocols, and influence on virtual screening enrichments. Journal of computer-aided molecular design, 2013, **27**, 221-234.

[42] Schrödinger Suite 2015-3 Protein Preparation Wizard; Epik version 3.3, Schrödinger, LLC, New York, NY, 2015; Impact version 6.8, Schröödinger, LLC, New York, NY, 2015; Prime version 4.1, Schrödinger, LLC, New York, NY, 2015.

[43] LigPrep, version 3.5, Schrödinger, LLC, New York, NY, 2015

[44] Farid, R., Day, T., Friesner, R. A., Pearlstein, R. A. New insights about HERG lockade obtained from protein modeling, potential energy mapping, and docking studies. Bioorganic & medicinal chemistry, 2006, **14**, 3160-3173.

[45] Schrödinger Suite 2015-3 Induced Fit Docking protocol; Glide version 6.8, Schrödinger, LLC, New York, NY, 2015; Prime version 4.1, Schrödinger, LLC, New York, NY, 2015.

[46] Osman, A.G., Elokely, K.M., Yadav, V.K., et. al. Bioactive products from singlet oxygen photooxygenation of cannabinoids. European Journal of Medicinal Chemistry, 2018, **143**, 983-996.

[47] Friesner, R. A., Murphy, R. B., Repasky, M. P., et. al. Extra precision glide: docking and scoring incorporating a model of hydrophobic enclosure for protein-ligand complexes. Journal of medicinal chemistry, 2006, **49**, 6177-6196.

[48] Bowers, K. J., Chow, E., Xu, H., et. al. In Scalable algorithms for molecular dynamics simulations on commodity clusters, SC Conference, Proceedings of the ACM/IEEE, 2006 pp 43-43.

[49] Shivakumar, D., Williams, J., Wu, Y., et. al. Prediction of absolute solvation free energies using molecular dynamics free energy perturbation and the OPLS force field. Journal of chemical theory and computation, 2010, **6**, 1509-1519.

[50] Desmond Molecular Dynamics System, version 4.3, D. E. Shaw Research, New York, NY, 2015. Maestro-Desmond Interoperability Tools, version 4.3, Schrödinger, New York, NY, 2015.

[51] Guo, Z., Mohanty, U., Noehre, J., et. al. Probing the α-Helical Structural Stability of Stapled p53 Peptides: Molecular Dynamics Simulations and Analysis. Chemical biology & drug design, 2010, **75**, 348-359.

[52] Tuckerman, M.E., Berne, B.J. Molecular dynamics algorithm for multiple time scale: Systems with disparate masses. J Chem. Phys., 1991, **94**, 1465.

[53] Martyna, G.J., Klein, M.L., Tuckerman, M.E. Nose hoover Chains: The canocial ensemble via continuous dynamics, J. Chem. Phys., 1992, **97**, 2635.

[54] Martyna, G.J., Tobias, D.J., Klein, M.L., Constant pressure molecular dynamics algorithms. J. Chem. Phys. 1994, **101**, 4177-4189.

[55] Cavasotto, C.N., Phatak, S.S., Homology modeling in drug discovery: current trends and applications. Drug discovery today, 2009, **14**, 676-683.

[56] Dhopeshwarkar, A., Mackie, K., CB2 Cannabinoid Receptors as a Therapeutic Target—What Does the Future Hold. Mol Pharmacol. 2014, **86(4)**, 430-437.

[57] Malan, P.T., Ibrahim,, M.M., Deng, H., et. al., CB2 cannabinoid receptor-mediated peripheral antinociception, Pain 2001, **93**, 239-245.

[58] Aung, M.M., Griffin, G., Huffman, J.W., et. al. Influence of the N-1 alkyl chain length of cannabimimetic indoles upon CB1 and CB2 receptor binding. Drug Alcohol Depend, 2000, **60 (2)**, 133-140.

[59] Frost, J.M., et al., Indol-3-ylcycloalkyl Ketones: Effects of N1 Substituted Indole Side Chain Variations on CB2 Cannabinoid Receptor Activity. Journal of Medicinal Chemistry, 2010, **53 (1)**, 295-315.